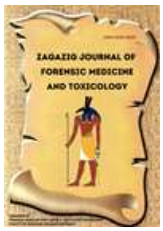

Zagazig Journal of Forensic Medicine and Toxicology 2025; 23(1): 158- 172

Zagazig Journal of Forensic Medicine and Toxicology

Journal homepage: https://zjfm.journals.ekb.eg/

Original article

Determination of the Burned Skin Injury Vitality and Its Postmortem Changes through Detection of Mir-711 and Mir-21 and Histopathological Changes in Adult Albino Rats

Mariam Nasrallah Gergis Ghobrial, Atef Abd El-Aziz Fouda, Sahar M. Abo El Wafa, Noha Elnajjar, Omima R. Mohamed

Department of Forensic Medicine and Clinical Toxicology, Faculty of Medicine, Benha University, Egypt.

ARTICLE INFO

Article history

Received: 21- 10- 2024
Revised: 25- 1- 2025
Accepted: 12- 2- 2025

Keywords: Burn, Vitality, Mir-21, Mir-711; Histopathology, postmortem interval

Abstract

Background: It is crucial to conduct a wound examination during the evaluation of a burned body. This is more pronounced when distinguishing between burns inflicted shortly before and after death. Nevertheless, the conventional findings of antemortem burns are usually nonspecific. **Objectives:** Verifying the ability of Mir-21 and Mir-711 expressions in skin and histopathological changes in skin and brain to determine vitality and estimate the postmortem interval (PMI) of cutaneous thermal burns. **Methodology:** Adult albino rats were used. Rats were randomly assigned to one of three groups: Group I: Samples were collected before and at the 0 time point after the rats' sacrifice. Group II: Burns were inflicted on the rats' skin, and then all rats were sacrificed after 30 minutes; samples were collected at 0, 12, 24, and 48 hours. Group III: Burns were inflicted on the rats' skin 30 minutes after sacrifice. **Results:** The antemortem burned regions exhibited elevated expressions of both Mirs compared to those of postmortem unburnt controls and postmortem burn samples. Mir-21 expression at 12 hours after death and Mir-711 at 24 hours after death were significantly higher than at other time intervals in Group II. Mir-21 expression in skin can be used to determine the vitality of cutaneous thermal burns up to 2 days after death, but Mir-711 can be used for only 1 day. Inflammatory cell infiltration in the skin and brain can be used as histopathological indicators of cutaneous thermal burns. **Conclusion:** The determination of the vitality of burned skin may be facilitated by the detection of Mir-21 and Mir-711 expressions. Histopathological signs of acute inflammation were detected in the brain and skin up to two days after the rats' death. The combination of multiple markers can be used to confirm PMI estimation in cutaneous thermal burns

DOI: 10.21608/ZJFM.2025.329684.1203
*Corresponding author: ***Mariam Nasrallah Gergis Ghobrial***
Email address: mariamnasrallah777333@yahoo.com

I. Introduction:

It is crucial to conduct a wound examination during the evaluation of a burned body (Lyu et al., 2018). The most challenging problem is distinguishing between burns inflicted shortly before and after death. Nevertheless, conventional findings for the identification of antemortem burns are usually nonspecific or nonexistent. Consequently, the establishment of new indicators for burn vitality is necessary (Zhang et al., 2020).

Burn injuries encompass scalds, contact burns, friction burns, electrical burns, and chemical burns, and their severity and intensity are contingent upon the extent of the burn on the body's surface area and the depth of the burn (Allahham et al., 2024).

Several studies have been conducted to ascertain the vitality of wounds; the majority of these studies have concentrated on proteins and microRNAs (Mirs). The nature of the lesion can be estimated through a variety of macroscopic and microscopic alterations. However, it is crucial to investigate the lesion using histological and biomolecular techniques, such as Mir analysis, due to the unascertained and variable results of the gross examination (Vinay et al., 2017; Madea, 2019).

Mir-21 is induced after skin injury, where it facilitates wound healing and maintains a high level of expression in the affected region (Long et al., 2018). While Mir-711's primary function is to regulate cell proliferation, apoptosis, and the cell cycle (Zhu et al., 2017).

The cutaneous reaction to heat, which results in vital reactions, blister formation, and microscopic examination of the tissues from the burned area, has been deemed very important (Chawla et al., 2014). Burn injuries have an impact on more than just the skin. One consequence of burn injuries is the impact on the central nervous system. It has long been acknowledged that cerebral disorders are a prevalent issue among patients who have sustained thermal injuries. Significant pathological changes in the brain, including severe edema and diffuse parenchymal hemorrhage, have also been observed in both animal studies and at autopsy. Over the past two decades, there has been a significant amount of research conducted on brain injury following burns (Chen et al., 2023).

The termination of physiological processes that maintain the integrity and functionality of cells is referred to as death. PMI is the time frame between the time of an individual's demise and the discovery of their corpse (Umapathi et al., 2023). The significance of estimating the PMI is not only due to its scientific relevance but also to the weight it conveys within the forensic field, which has clear legal implications (Dell'Aquila et al., 2021).

We therefore aim to assess the vitality and estimate the PMI of cutaneous thermal injury by examining the expression of Mir-21 and Mir-711 in the skin, as well as the histopathological alterations in the skin and the brain.

II. Material and Methods

II.1 Setting and ethical considerations:

This study is a prospective animal model conducted at the Faculty of Medicine, Benha University, in the departments of Forensic Medicine and Clinical Toxicology, Medical Biochemistry and Molecular Biology, and Pathology. It adhered to the Guidelines for the Care and Use of Laboratory Animals (Clark et al., 1997), and the protocol was authorized by the Local Ethical Committee at the Faculty of Medicine, Benha University, under approval code (Ms-28-6- 2023).

The Study Animals: The study comprised 36 adult albino rats that were robust and grew normally, with a weight of 200-250 grams. The animals were procured from The Animal Farm and grown in the Animal House at the Faculty of Veterinary Medicine, Benha University, for a period of two weeks prior to the commencement of the experiment to gradually adapt to the new farming conditions. Rats were maintained in standard living conditions, with a temperature of 20°C, a humidity rate of 60%, and a 12-hour day/night cycle, and were provided with a standard diet and free access to water.

II.2 Methods:

Antemortem burn infliction: Rats were anesthetized by 1.9% diethyl ether inhalation in a glass cage according to Johns Hopkins University (JHU) guidance on the use of ether for animal anesthesia, and subsequently shaven to expose the skin area using an electric razor. The dorsal skin was subjected to a 30 mm × 10 mm sheet of copper that was heated to 100°C for a duration of 4 seconds. The rats' back skin was subjected to partial thickness burn as

a result of this procedure (Lyu et al., 2018), covering 15% of the total body surface area (TBSA). All rats were sacrificed after 30 minutes by cervical decapitation after being anesthetized with diethyl ether and maintained at 24°C.

Postmortem burn infliction: After shaving the dorsal hairs, the rats were instantaneously sacrificed by cervical decapitation after being anesthetized with diethyl ether. Thirty minutes after death, the same heated copper sheet was used to apply dorsal skin burns for a duration of 4 seconds.

Specimen harvesting: Two skin samples (one for evaluation of Mir expression and the other for histopathology) measuring 5 mm × 5 mm (whether burnt or not, according to the group) together with brain tissue samples were obtained at the predetermined time points in each group.

II.3 Grouping: The animals were assigned to one of three groups (total n = 36):

Group I (Control group) (n=6): Rats were left without burns to serve as the control. Skin samples were obtained while alive as antemortem control samples and at the 0 time point after the rats' death as postmortem unburnt control samples. Brain samples were obtained after the rats' death as postmortem control samples.

Group II (Antemortem burn group) (n=24, 6 for each time interval): The antemortem burned skin and brain samples were obtained at 0, 12, 24, and 48 hours after the rats' death.

Group III (Postmortem burn group) (n=6): The postmortem burned skin and brain samples were obtained at the 30-minute time point after the rats' death.

II.4 Samples Preservation:

Skin samples for evaluation of Mir expression: Immediately after sample collection, they were placed in a dry sterile clean tube containing normal saline and kept frozen at -80°C until further processing.

Skin and brain samples for histopathological examination: These were placed in 10% formalin until further processing.

II.5 Estimation of expression levels of Mir-21 and Mir-711: After sampling and preservation of the skin samples:

Mir extraction: The RNA, including Mirs, was extracted from all skin samples using the RNeasy mini kit according to the manufacturer's instructions, Qiagen GmbH, Germany. Spectrophotometric quantification of RNA was performed using a Nanodrop spectrophotometer (USA) with measurements at A_{260} and A_{280}. The concentration of RNA samples was measured at 44 µg/ml at A_{260} (Wilfinger et al., 1997). The ratio of the reading at A_{260}/A_{280} provides an estimate of the purity of RNA. Pure RNA has an A_{260}/A_{280} ratio of 1.9 to 2.1. The Mir-21 and Mir-711 were amplified using a Real-Time PCR machine (Step One, Applied Biosystems (ABI), USA) with Glyceraldehyde 3-phosphate dehydrogenase (GAPDH) as a housekeeping gene, using specific primer sequences (Table 1)

Table (1): Shows primer sequences of Mir-21, Mir-711 and GAPDH.

Mirs	Primer sequence	Reference
Mir-21	Forward Sequence: 5′-AGCTTATCAGACTGATGTTG-3′ Reverse Sequence: 5′-GAACATGTCTGCGTATCTC-3′	M10000569 ID:387140 (OriGene.com)
Mir-711	Forward Sequence: 5′-GGGACCCTGGGAGAGATGT-3′ Reverse Sequence: 5′-GAACATGTCTGCGTATCTC-3′	M10012621 ID:100314143 (OriGene.com)
GAPDH	Forward Sequence: 5′-CATCACTGCCACCCAGAAGACTG-3′ Reverse Sequence: 5′-ATGCCAGTGAGCTTCCCGTTCAG-3′	NM_008084 ID:14433 (OriGene.com)

MiR: microRNA, GAPDH: glyceraldehyde 3- phosphate dehydrogenase

The amplification steps were as follow:

1. Conversion of Mir to cDNA using Soliscript ® RT cDNA Synthesis MIX according to manufacturer instructions.
   - In Veriti 96 well Thermal cycler ABI (USA) machine according to the following protocol (table 2).
2. The amplification master mix using HERA PLUS SYBR Green QRT-PCR Kit Willowfort (WF1030800X).
3. Analysis of the amplified products using step one program analysis.

Table (2): Shows reaction components in a nuclease-free microcentrifuge tube.

Component	Volume	Final concentration (20 µL)
Template RNA	8 µL	,1 ng - 1µg
10x RT reaction premix without primers	2 µL	1x
Gene specific primer	1µL	.1- 1µM
SOLIScript Enzyme Mix	1,5 µL	
Nuclease-free H_2O	8,5 µL	
Total	20 µL	

RNA: ribonucleic acid, RT: reverse transcription.

- For which we used the following program (table 3).

Table (3): Shows program for cDNA synthesis.

Step	Temperature	Time
Reverse transcription	50°C	30 minutes
Enzyme inactivation	85°C	5 minutes

Calculation of the Results:

Mir-21 and Mir-711 quantification: The expression levels of mir-21 and mir-711 were calculated for the two burn groups and the control group. The housekeeping gene, GAPDH, is commonly used as a reference gene for normalization because its expression levels remain relatively stable. It was calculated for both burn groups and the control group. Fold change or relative quantity was calculated using the formula of fold change = 2^(-ΔΔCT) method (Livak and Schmittgen, 2001).

2^(-ΔΔCT) Method: This method has been extensively used as a relative quantification strategy for quantitative reverse transcription real-time polymerase chain reaction (qRT-PCR) data analysis. The threshold cycle (CT) is the cycle at which the fluorescence level reaches a certain threshold. This method directly uses the CT information generated from a qRT-PCR system to calculate relative gene expression in target and reference samples, using a reference gene as the normalizer.

The delta CT was calculated using: $\Delta CT = CT$ (target gene) – CT (reference gene). The difference between the burn and the control tissue delta CT (delta-delta CT) was calculated using: $\Delta\Delta CT = \Delta CT$ (target sample) $-\Delta CT$ (reference sample). The final result of this method is presented as the fold change of target gene expression in a target sample relative to a reference sample, normalized to a reference gene.

II.6 Histopathological examination of skin and brain samples: Sections were examined at the Pathology Department, Faculty of Medicine, Benha University. The tissue samples were stained with Hematoxylin and Eosin (H&E) according to Suvarna et al. (2018) and examined using a light microscope (OLYMPUS, Japan) for histopathological alterations along defined times in each group to determine vitality and to provide a scorecard for PMI estimation as follows:

For skin samples in Group II: Each slide was evaluated for the following: the degree of inflammatory cell infiltration, edema, hemosiderin deposition, fibrous tissue, and collagen deposition to determine the effect of PMI on scoring of the skin histopathological picture in rats' antemortem burn according to Ibrahim et al. (2019).

For brain samples in Group II: Each slide was evaluated for the following: the degree of inflammatory cell infiltration, perivascular astrocytes, swelling of endothelial cells, vacuolations in neurons, and gliosis to determine the effect of PMI on scoring of the brain histopathological picture in rats' antemortem burn, guided by our histopathological findings and scorecard developed by Ibrahim et al. (2019).

Regarding scoring in Group II: The absence of histological findings was denoted by (–) and given a score of zero, whereas + was given a score of 1, ++ was given a score of 2, and +++ was given a score of 3 for mild, moderate, or marked changes, respectively, with less than 25%, 50%, and 75% affection of the total fields examined. Data were collected from skin and brain tissue sections from each animal, with three fields per section (n = 3).

II.7 Statistical analysis:

The software used for statistical analyses was PSW (20), IBM Corp., Released 2011, Version 24.0 of IBM SPSS Statistics for Windows (IBM Corp., Armonk, NY). Means ± standard deviation were used for parametric quantitative data, while the median, minimum, and maximum were used to express non-parametric quantitative data. The Kolmogorov-Smirnov and Shapiro-Wilk tests were implemented to evaluate the normality of numerical data. The significance of numerical data between the three groups was assessed using the ANOVA test (F) (Analysis of Variance), according to the normality of distribution. The Friedman test ($F(X^2)$) or the repeated measures ANOVA test (F) were used for the four repeated measures of numeric variables. Different possible cutoffs for the diagnostic marker were employed to evaluate its efficacy as a diagnostic tool using ROC curves. The Spearman correlation was employed to measure the intensity and direction of the relationship between two non-parametric variables. Statistical significance was determined when the P value was less than 0.05 (Peacock and Peacock, 2020).

III-Results:

Assessment of Mir expressions in skin samples:

In Group I, Mir-21 and Mir-711 both decreased after death, but Mir-711 was highly significantly decreased when compared to its level before death (P = 0.002).

In Group II, Mir-21 and Mir-711 expressions at the 0 time point after death were highly significantly increased ($p < 0.01$) compared to postmortem unburnt control samples of Group I and Group III (Figure 1).

Mir-21 expression (12 hours after death) and Mir-711 (24 hours after death) were highly significantly increased compared to other time intervals in Group II ($p < 0.01$ for both). Mir-21 expression at 48 hours remained highly significantly decreased compared to the level at 0 time ($p < 0.01$), while Mir-711 at 48 hours was highly significantly decreased compared to the level at 0 time ($p < 0.01$) (Figure 2).

Histopathological examination of skin and brain

A. Skin Sections:

Group I: Skin sections showed normal histologic architecture of samples taken before and after the rats' death without burn (Figure 3A, B).

Group II: Skin sections exhibited the following changes:

At 0 Time Point: Coagulative necrosis of the dermis and epidermis, epidermal separation, vesicle formation, mild inflammatory cell infiltration (neutrophils and mononuclear cells, primarily macrophages), congestion and dilation of capillaries with blood extravasation, absent or mild edema, pyknotic epidermal nuclei, and vacuolation of cells (Figure 3C).

At 12 Hours: Advanced degree of inflammatory cell infiltration, mild to moderate edema, myxoid degeneration, and moderate degree of autolysis of dermal structures (Figure 3D).

At 24 Hours: No inflammatory cells, edema almost disappeared, foci of dermal collagen and fibrous tissue formation, and severe degree of autolysis of dermal structures (Figure 3E).

At 48 Hours: Increased dermal fibrosis, evident hemosiderin, and severe degree of autolysis of dermal structures (Figure 3F).

Group III: Skin sections showed coagulative necrosis, vesicle formation, pyknotic nuclei, and separation of the

epidermis, but no inflammatory cell infiltration, nor congestion or dilation of capillaries (Figure 3G).

Impact of PMI Duration on Scoring:

The scoring of the skin histopathological picture in the antemortem thermal burn of rats in Group II was as follows (Table 4):

- Skin score at 0 time point ranged from 1 to 3 with a median value of 2.
- At 12 hours, it ranged from 4- 6 with a median value of 5.
- At 24 hours, it ranged from 0- 2 with a median value of 1.
- At 48 hours, it ranged from 4-6 with a median value of 5.

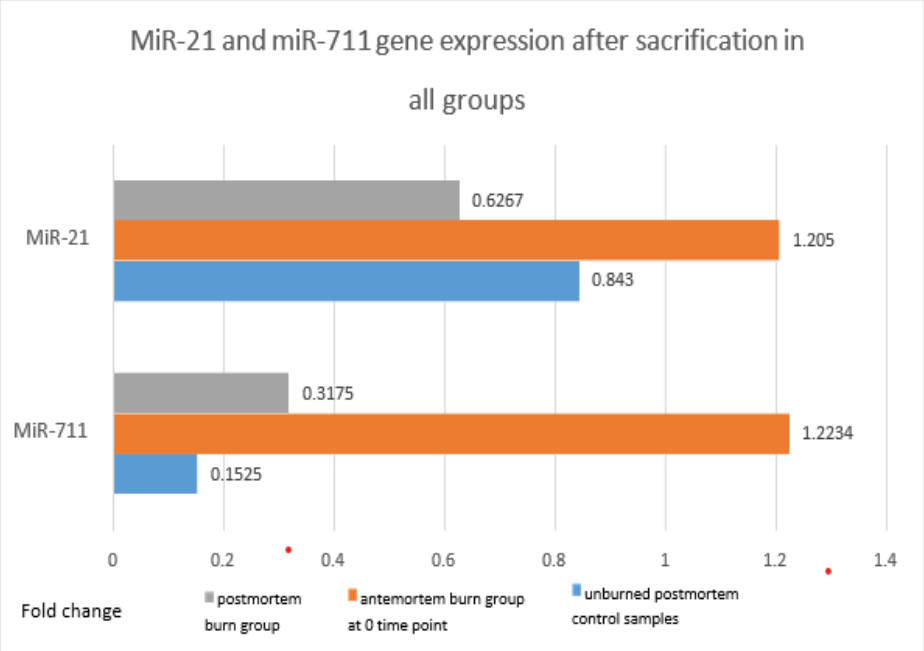

Figure (1): Mir-21 and Mir-711 gene expressions in the studied groups.

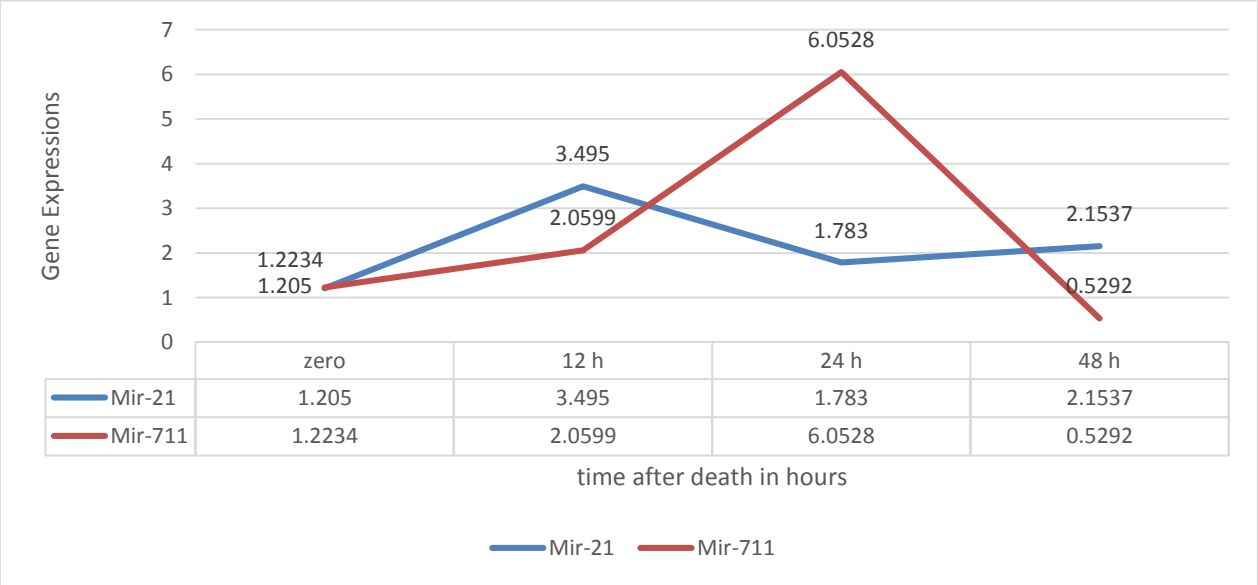

Figure (2): Mir-21 and Mir-711 gene expressions at different postmortem time intervals in Group II

Table (4): Effect of postmortem interval on total scoring of the brain histopathological picture in rats' thermal burn in Group II using the Friedman test.

Parameters	At zero time	After 12 h	After 24 h	After 48h	Test of significance	P value
Skin score						
Mean ± SD	2.00±0.894	5.0±0.632	1.0±0.632	5.0±0.632	F(X2) = 19.135	0.000**
Min-Max	2 (1-3)	5 (4-6)	1 (0 -2)	5(4- 6)		

SD: standard deviation, Min: Minimum, Max: Maximum, F(X2): Friedman test, **: highly significant at p < 0.01

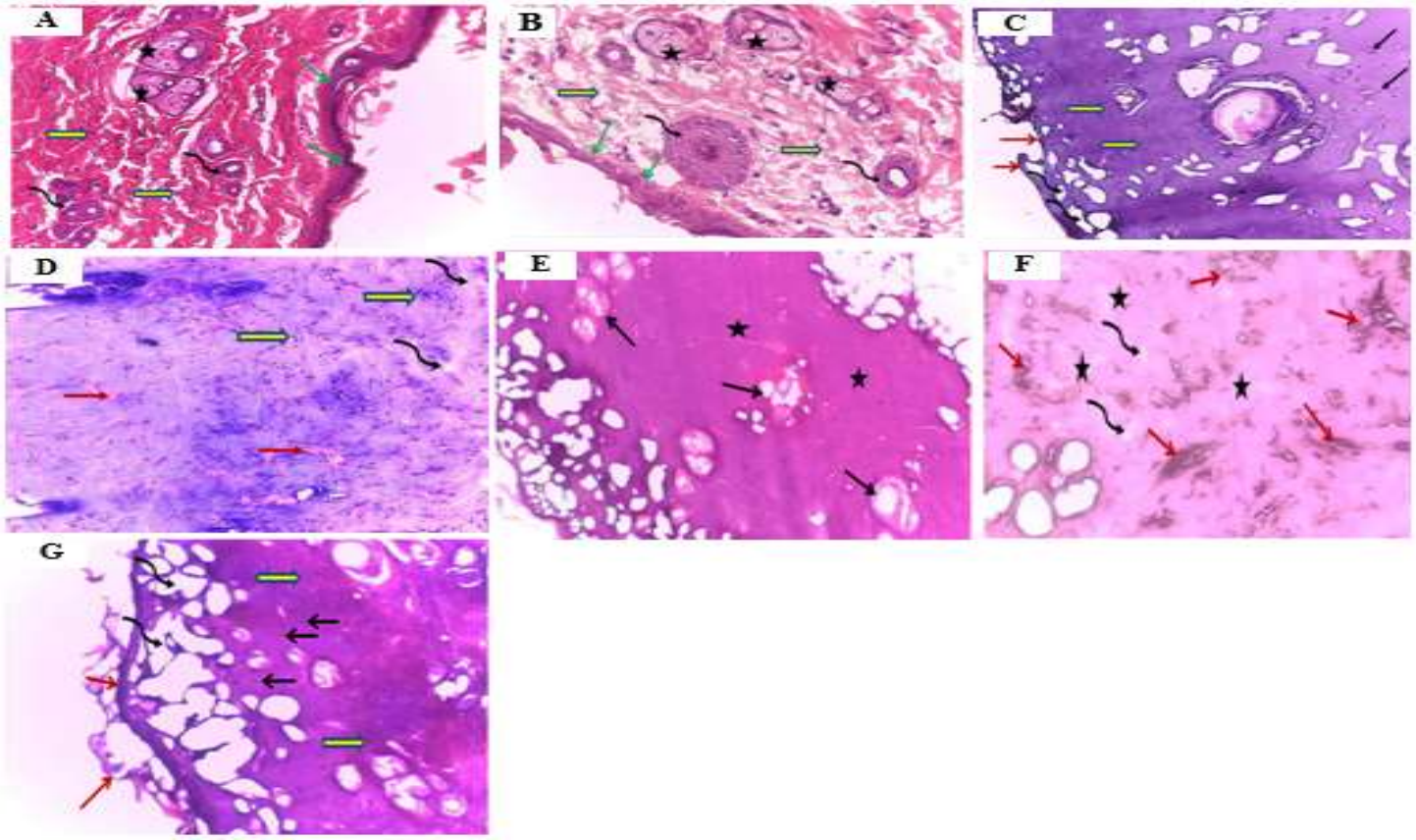

Figure 3: A, B: Two photomicrographs of sections from the antemortem and postmortem unburnt control group skin, respectively, showed normal skin histoarchitecture. Thin epidermis (green arrows) and thick dermal layer of collagenous connective tissue (block yellow arrows) contain hair follicles (curved black arrows) and sebaceous glands (stars) (H&E x20, H&E x40) respectively. C, D, E, F: Four photomicrographs of sections from rats' skin of Group II.

- C: At 0 time point after rats' death, showed coagulative necrosis (block yellow arrows), separation of epidermis (red arrows), vesicle formation (curved black arrows), and mild inflammatory cell infiltration (black arrows) (H&E x20).
- D: At 12 hours after rats' death, showed advanced degree of inflammatory cell infiltration (block yellow arrows), myxoid degeneration (red arrows), and advanced degree of edema (curved black arrows) (H&E x20).
- E: At 24 hours after rats' death, showed foci of fibrous tissue formation and dermal collagen deposition (stars), and severe degree of autolysis of hair follicles (black arrows) (H&E x40).
- F: At 48 hours after rats' death, showed marked dense dermal fibrosis and collagen deposition (stars), mild edema (curved black arrows), with hemosiderin deposition (red arrows) (H&E x40).

G: A photomicrograph of a section from a rat's skin of Group III showed coagulative necrosis (block yellow arrows), separation of epidermis (red arrows), vesicle formation (curved black arrows), and pyknotic nuclei (black arrows) (H&E x20).

B. Brain Sections:

Group I: Brain sections showed normal histologic architecture of nerve cell bodies, surrounding supportive cells, and neuropil in all specimens taken (Figure 4A).

Group II: Skin sections exhibited the following changes:

At 0 Time Point: Mild to moderate swelling of endothelial cells, mild vacuolation of neurons, a moderate degree of dispersed inflammatory cell infiltration (neutrophils and mononuclear cells, primarily macrophages), and mild degree of gliosis (Figure 4B).

At 12 Hours: Mild to moderate swelling of endothelial cells, moderate vacuolation of neurons with condensation of nuclei, moderate degree of dispersed inflammatory cell infiltration, moderate degree of gliosis, and mild degree of perivascular astrocytes (Figure 4C).

At 24 and 48 Hours: Moderate degree of endothelial cell swelling, moderate to marked vacuolation of neurons with condensation of nuclei, marked inflammatory cell infiltration with abscess formation (clustered leukocytes), moderate degree of gliosis, and mild to moderate degree of perivascular astrocytes (Figure 4D, E).

Group III: Brain sections showed vacuolation of neurons in all specimens taken. There were no inflammatory cell infiltrates or gliosis (Figure 4F).

Impact of PMI Duration on Scoring: The scoring of the brain histopathological picture in the antemortem thermal burn of rats in Group II was as follows (Table 5):

- Brain score at 0 time ranged from 3- 5 with a median of 4.
- At 12 hours, it ranged from 8- 9 with a median value of 8.
- At 24 hours, it ranged 9- 12 with a median value of 11.
- At 48 hours, it ranged 11- 12 with a median value of 12.

Table (5): Effect of postmortem interval on total scoring of brain histopathological picture in rats' thermal burn in group II using Friedman test.

Parameters	At zero time	After 12 h	After 24 h	After 48h	Test of significance	P value
Brain score						
Mean ± SD	3.83±0.753	8.17±0.408	10.83±0.983	11.83±0.408	F(X2) = 21.088	0.000**
Min-Max	4 (3-5)	8 (8-9)	11 (9-12)	12 (11-12)		

SD: standard deviation, Min: Minimum, Max: Maximum, F(X2): Friedman test, **: highly significant at $p < 0.01$

Receiver Operator Characteristic (ROC) curves, sensitivity, specificity, and accuracy of differential microRNA expressions and histopathological scores in Group II:

Between 0 time and 12 hours after death: At combined cutoff points of 2.2875 for Mir-21, 1.6835 for Mir-711, 3.5 for skin score, and 6.5 for brain score, these yielded a sensitivity of 100%, specificity of 100%, and accuracy of 100%, indicating that this sample passed 12 hours after the rats' death (Figure 5A).

Between 0 time and 24 hours after death: At combined cutoff points of 1.4155 for Mir-21, 3.614 for Mir-711, and 7 for brain score, these yielded a sensitivity of 100%, specificity of 100%, and accuracy of 100%, indicating that this sample passed 24 hours after the rats' death, while the skin score was insignificantly different from the 0-time score (Figure 5B).

Between 0 time and 48 hours after death: At combined cutoff points of 1.629 for Mir-21, 3.5 for skin score, and 8 for brain score, these yielded a sensitivity of 100%, specificity of 100%, and accuracy of 100%, indicating that this sample passed 48 hours after the rats' death in Group II. However, at a cutoff point of 0.808 for Mir-711, which is significantly decreased from the 0-time level of 1.2234±0.131 and control level of 0.1525±0.0032, this resulted in 0% sensitivity, 0% specificity, and 0% accuracy as it completely dropped below both the 0-time level and control level (Figure 5C).

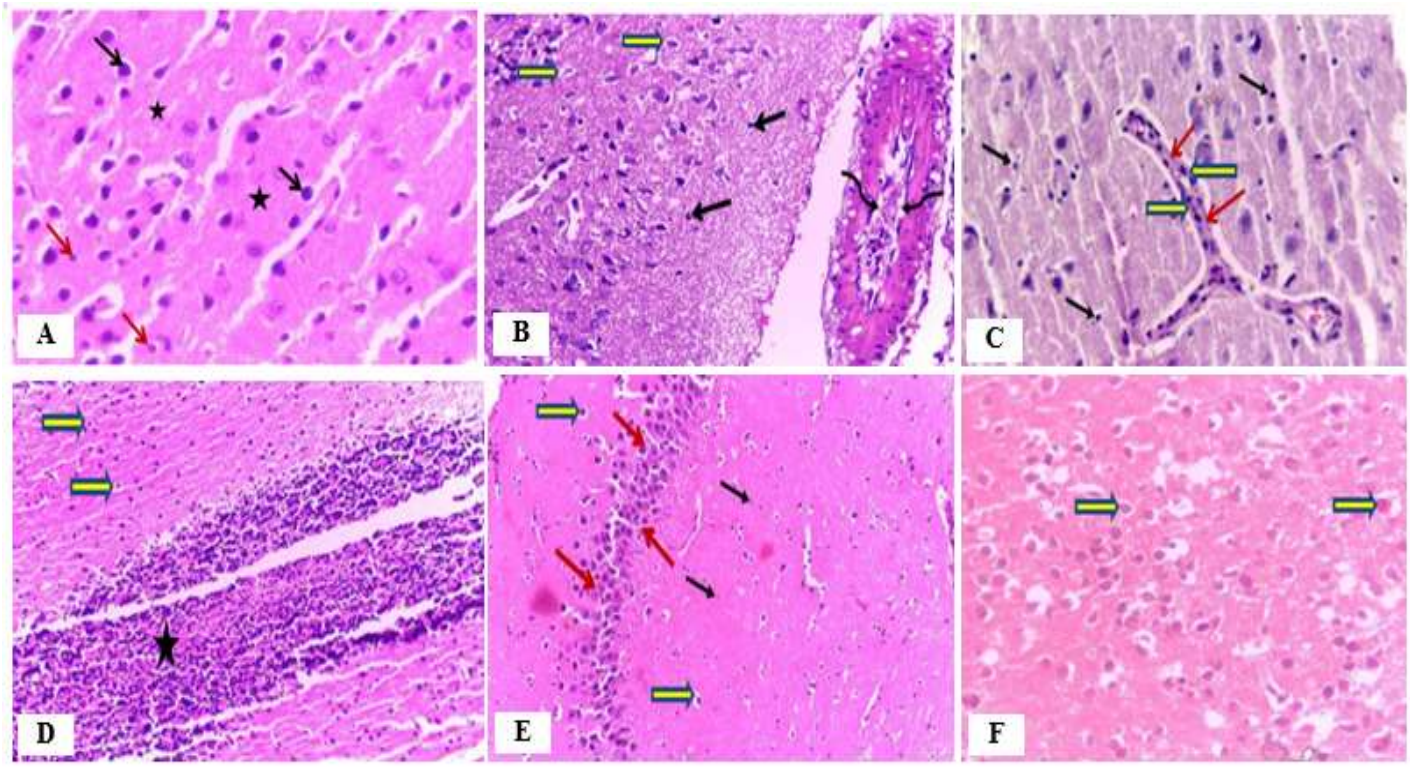

Figure 4: A: A photomicrograph of a section from a rat's cerebrum of the control group showed normal histological structures of the cerebral cortex, including nerve cell bodies (black arrows), surrounding supportive cells (red arrows), and neuropil(stars)(H&Ex40). B, C, D, E: Four photomicrographs of sections from rats' cerebrum of Group II.

- B: At 0 time point after the rat's death, showed mild swelling of endothelial cells (curved black arrows), vacuolation of neurons (block yellow arrows), and mild inflammatory cell infiltration (black arrows) (H&E x40).
- C: At 12 hours after the rat's death, showed mild swelling of endothelial cells (red arrows) with mild degree of perivascular astrocytes (block yellow arrows) and dispersed inflammatory cell infiltrates (black arrows) (H&E x40).
- D: At 24 hours after the rat's death, showed abscess formation (clustered leukocytes) (star) and vacuolation of neurons with condensation of nuclei (block yellow arrows) (H&E x20).
- E: At 48 hours after the rat's death, showed moderate degree of gliosis (red arrows), marked vacuolation of neurons with condensation of nuclei (block yellow arrows), and dispersed leukocytes (black arrows) (H&E x20).

F: A photomicrograph of a section from a rat's cerebrum of Group III showed mild vacuolation of neurons (block yellow arrows) (H&E x40).

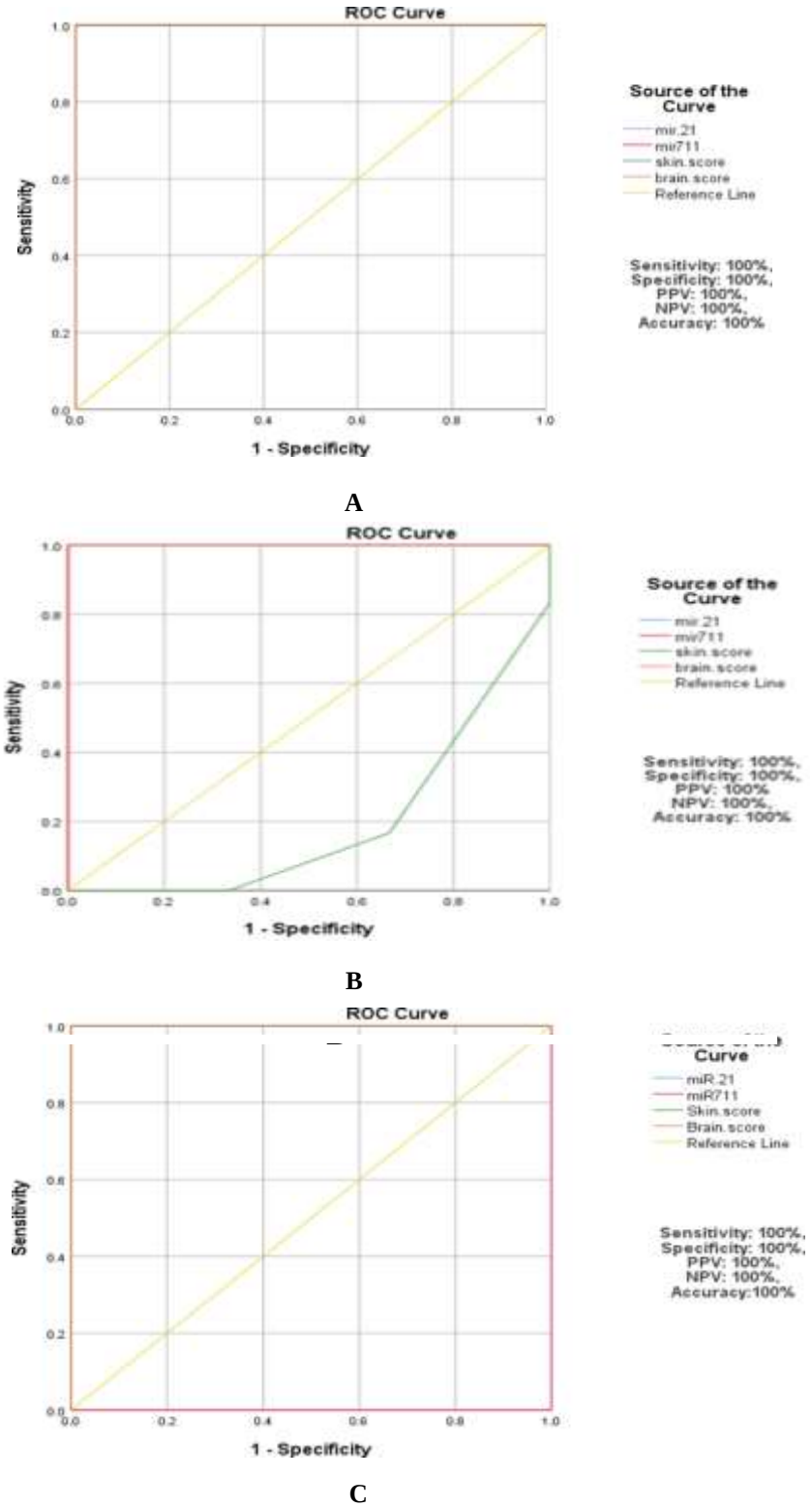

Figure 5: Illustrates the ROC curves, sensitivity, specificity, and accuracy of the differential microRNA expressions and histopathological scores of Group II. A: Between 0 time and 12 hours after death. B: Between 0 time and 24 hours after death, C: Between 0 time and 48 hours after death

Effect of PMI on both microRNAs' expressions and histopathological scores in Group II:

At short durations after death, up to 24 hours, a significant moderate positive correlation was observed between time and Mir-21, as well as significant strong positive correlations between both Mir-711 and brain score with time. However, no significant correlation was observed with skin score. At longer durations after death, up to 48 hours, there was no significant correlation with Mir-21, Mir-711, or skin score, while a significant positive correlation was observed between brain score and time (Table 6).

Table 6: Spearman correlation between microRNA expressions and histopathological scores with time up to 24 hours and up to 48 hours after death in Group II:

Variable	Time intervals			
	Up till 24 h		Up till 48 h	
	R	P value	R	P value
Mir-21	0.427	0.048*	0.371	0.074
Mir-711	0.944	0.000**	0.194	0.364
Skin score	-0.296	0.233	0.277	0.190
Brain score	0.959	0.000**	0.955	0.000**

R: Spearman's rho correlation coefficient, Mir: microRNA. *: Significant at $p < 0.05$, **: Highly significant at $p < 0.01$.

IV-Discussion

The identification of antemortem and postmortem burns is extremely important in the field of forensic pathology. Upon the discovery of a corpse at a fire scene, a forensic pathologist needs to determine whether the individual was alive upon sustaining the burns and whether the death was caused by thermal injury (Zhang et al., 2020).

In our study, we evaluated vitality, molecular, and histopathological changes in antemortem cutaneous thermal burn injury that occurred shortly before death. Additionally, we provided a histo-biomolecular approach to estimate PMI.

MicroRNAs (Mirs) are very short nucleic acids that can withstand high temperatures and pH levels. Extracted Mirs are stable at room temperature for one year and remain detectable in storage at -20°C for a period of ten years (Grasedieck et al., 2012). miRs have also shown continued expression in several studies at postmortem intervals (Dell'Aquila et al., 2021).

The histopathological findings of burns are initially caused by the direct effects of thermal injury and subsequently by the inflammatory healing response (Malik et al., 2021). The early postmortem interval can be determined by observing the sequential histopathological changes (Surendhar et al., 2023). Examination of genetic expression and histopathological evaluation provides recent methods of PMI estimation (Welson et al., 2021).

Our study followed the same burned skin model as Lyu et al. (2018) and Zhang et al. (2020) with a total body surface area (TBSA) affected of 15%. The levels of Mir-21 and Mir-711 were higher in the antemortem burned regions than in the postmortem control samples and in postmortem burns.

In accordance with these results, Zhu et al. (2014) and Guo et al. (2017) confirmed through QRT-PCR analysis that Mir-21 was up-regulated in hypertrophic scar tissue obtained from burn patients and cultured hypertrophic scar fibroblasts. Furthermore, Long et al. (2018) studied the impact of Mir-21 on the wound healing process in aged mice. They discovered that Mir-21 expression remained high in the wounded area, facilitating skin repair capabilities. Additionally, they asserted that its dysregulation may be responsible for the impairment of wound repair.

In agreement with our results, Lyu et al. (2018) and Zhang et al. (2020) found that the levels of Mir-711 and Mir-183-3p were significantly elevated in the antemortem burned mouse skin, which is consistent with our findings. Furthermore, Zhang et al. (2020) discovered that the levels of these two Mirs were significantly higher in the burned regions of 19 cases compared to intact regions using human burned skin specimens.

miR-21 expression in skin can be used for the determination of the vitality of antemortem cutaneous

thermal burns up to 2 days after death when compared to Mir-711. This is due to the fact that Mir-21 is one of the most highly conserved Mirs that have been identified (Jenike and Halushka, 2021).

Continuous expression of Mir-205 and Mir-21 was observed in skin samples obtained from cutaneous incisional wounds up to 2 days after death by Ibrahim et al. (2019). This is in agreement with our results.

Zhang et al. (2020) discovered that elevated Mir-711 and Mir-183-3p levels could still be observed until 5 days after death in antemortem burned regions of mouse skin. In contrast, these two Mirs' increased levels were detected only until 2 days after the autopsy of human skin. This indicates that Mir-711 expression in burnt skin requires further investigation regarding the duration for which it can be detected after death.

As the postmortem duration increases, molecular degradation in deceased individuals increases. Consequently, gene expressions undergo a consistent decline as the time following death increases. miRs are capable of resisting ribonuclease degradation due to their tight binding to the active RNA-induced silencing complex, playing special functions in keeping cells alive after death. Therefore, Mirs can be continuously expressed (Wang et al., 2016).

We did not demonstrate a significant negative correlation between Mir expressions and time up to 2 days after death. This is in agreement with Ibrahim et al. (2019), who did not find any statistically significant negative correlation between Mir expression and PMI up to 2 days after death. Conversely, this is at odds with the findings of other studies (Sampaio-Silva et al., 2013; Lv et al., 2014). These conflicting results may be attributed to the molecular molecule studied, the tissue examined, and the postmortem duration selected (Ali et al., 2017).

Regarding histopathological samples, acute inflammatory cells appeared immediately in antemortem burned skin, together with other local effects of heat. As the time since injury increased, antemortem burns exhibited deposition of collagen, fibrous tissue, and hemosiderin. In contrast, postmortem burned skin did not show any inflammatory cell infiltrate.

In agreement with our histopathological findings, Reddy and Murty (2017) showed that the histopathological examination of antemortem burned skin may reveal vital reactions microscopically. These histopathological findings were consistent with the studies conducted by Sangita et al. (2018) and El Euony et al. (2023) on dry thermal burns in rats and human skin samples, respectively. In line with our histopathological findings, Ibrahim et al. (2019) found a similar histopathological picture in their study on cutaneous incisional wounds at 0, 24, and 48 hours after death.

In cerebral cortex sections of the antemortem burn group, acute inflammatory cells and gliosis were immediately observed, along with signs of edema. Cerebral cortex sections exhibited perivascular astrocytes and microabscess formation as the time since injury increased. In contrast, postmortem burn brain samples did not exhibit any inflammatory cell infiltrate or gliosis.

The initial response to burn injury is systemic inflammation. This response can result in an increase in the levels of proteins and other inflammatory factors that are released, which can damage the extracellular matrix of the blood-brain barrier (BBB), contributing to cerebral edema by increasing BBB permeability (Allahham et al., 2024). Systemic neutrophils are then able to infiltrate the perivascular space freely as a result of the damaged BBB and increased microvascular permeability. Neutrophil infiltration into the brain is progressive, resulting in dispersed infiltration or microabscesses (Chi et al., 2021). Several studies have also suggested that the activation of microglia in the brain may be involved in neuroinflammation and neuronal apoptosis (Li et al., 2018; Ma et al., 2019).

In support of these histopathological findings, Zhang et al. (2011) showed that the invasion of dispersed or even clustered leukocytes in the cortex occurs as early as 8 hours post-burn. At the same time, neurons were shrunken with condensed nuclei, suggesting an early stage of apoptosis. Dispersed infiltration of leukocytes and even microabscesses were seen as late as 24 hours post-burn. Moreover, they demonstrated activation of microglia following this burn injury.

Our histopathological findings in skin and brain indicate that inflammatory cell infiltration in the skin and cerebral cortex can be used as histopathological indicators for cutaneous thermal burn injury vitality. This is consistent with the findings of Neri et al. (2018) and Salerno et al. (2022).

The need for histopathological scoring of wounds based on different parameters has been emphasized in many studies

of skin wound healing (Masson-Meyers et al., 2020). The utility of histopathological variation of the skin as an adjunct parameter for determining PMI in medicolegal cases was emphasized by Bardale et al. (2012). We developed a scorecard specifically tailored for the evaluation of burned skin samples and brain cerebrum samples of rats, based on the histopathological alterations documented in the aforementioned studies.

Statistical analysis revealed that the skin score did not show a positive correlation with the time passed since death. In contrast, the brain score showed a strong positive correlation with PMI, significantly increasing with time up to 48 hours after death in Group II.

Interestingly, our findings indicated that the diagnostic accuracy of PMI estimation could be enhanced by the combination of multiple markers. The skin score values in Group II were closely correlated at the 0- and 24-hour post-death time points, as indicated by the aforementioned score values. Similarly, they were closely related at the 12- and 48-hour time points after death. Subsequently, high Mir-21 expression and/or brain score at the 12-hour time point after death should be combined with the skin score at the same time point to provide an accurate estimation of PMI. Likewise, high Mir-711 expression and/or brain score at the 24-hour time point after death might distinguish between the closely related skin scores at the 0- and 24-hour time points after death. Finally, a high value of brain score at the 48-hour time point after death, when combined with the skin score at the same time point, can confirm an accurate estimation of PMI.

V-Conclusion

Using burned skin and brain samples from rats, the present study suggests that the detection of Mir-21 and Mir-711 levels may be useful for determining the vital reaction of burned skin. We demonstrated evidence that histopathological signs of acute inflammation in the skin and brain can be detected early in burn injury, starting from the time of infliction up to two days after death, and can be used as indicators of burn vitality. Nevertheless,

molecular changes became more pronounced in determining the time passed after death at 12 hours for Mir-21 and at 24 hours for Mir-711. The elevated Mir-21 level was still observed in antemortem burned skin until two days after death, while the elevated Mir-711 level was observed only until one day after death. Our results indicated that the combination of multiple markers might increase the accuracy of PMI estimation in cutaneous thermal burns.

VI. Recommendations and limitations

We recommend demonstrating Mir -21 and Mir -711 levels in human skin specimens retrieved from burn cases in further clinical research. A multimodal approach should be utilized: combining histopathological and Mir analyses to improve the accuracy of burn vitality assessment and PMI estimation. More research is needed into the histo- and biomolecular changes of antemortem burns occurring shortly before death within successive shorter intervals from different body sites to augment the preliminary results of this study.

Declarations

Sources of Funding

This work was self-funded by the corresponding author.

Ethical approval

The study was approved by Research Ethics committee (REC) of Faculty of Medicine, Benha University, Egypt under approval code (Ms-28-6- 2023).

Data availability statement

The datasets analyzed during the current study are available from the corresponding author on reasonable request.

Conflict of interest

The authors declared that there was no conflict of interest.

References:

Ali, M.M., Ibrahim, S.F. and Fayed, A.A., (2017): Using skin gene markers for estimating early postmortem interval at different temperatures. *The American Journal of Forensic Medicine & Pathology*, 38(4):323- 325. Doi: 10.1097/PAF.0000000000000337.

Allahham, A., Rowe, G., Stevenson, A., et al., (2024): The impact of burn injury on the central nervous system. *Burns & Trauma*, 12: tkad037. Doi: 10.1093/burnst/tkad037.

Bardale, R.V., Tumram, N.K., Dixit, P.G., et al., (2012): Evaluation of histologic changes of the skin in postmortem period. *The American Journal of Forensic*

Medicine and Pathology, 33(4):357-361. Doi: 10.1097/PAF.0b013e31822c8f21.

Chawla, R., Chawla, K., Sharma, G., et al., (2014): Differentiation of antemortem & postmortem burns by histopathological examination. *Journal of Forensic Medicine & Toxicology,* 31(2):70-74. Https://jfmtonline.com/index.php/jfmt/article/view/343.

Chen, J., Zhang, D. and Zhang, J., et al., (2023): Pathological changes in the brain after peripheral burns. *Burns & Trauma,* 11: tkac061. Doi: 10.1093/burnst/tkac061.

Chi, Y., Liu, X. and Chai, J., et al., (2021): A narrative review of changes in microvascular permeability after burn. *Annals of Translational Medicine,* 9(8):719. Doi: 10.21037/atm-21-1267.

Clark, J.D., Gebhart, G.F., Gonder, J.C., et al., (1997): Special Report: The 1996 Guide for the Care and Use of Laboratory Animals. *ILAR Journal,* 38(1):41-48. Doi: 10.1093/ilar.38.1.41.

Dell'Aquila, M., de Matteis, A., Scatena, A., et al., (2021): Estimation of the time of death: where we are now? *La Clinical terapeutica,* 172(2):109-112. Doi: 10.7417/CT.2021.2294.

El Euony, O.I., Wisely, Y.W., Nazem, A.M., et al., (2023): Histological, ultrastructural and genetic investigatory comparison between different types of experimentally - induced antemortem burns. *Journal of Forensic Science and Medicine,* 9(1):17-24. DOI: 10.4103/jfsm.jfsm_85_21.

Grasedieck, S., Scholer, N., Bommer, M., et al., (2012): Impact of serum storage conditions on microRNA stability. *Leukemia,* 26(11):2414-2416. Doi: 10.1038/leu.2012.106.

Guo, L., Xu, K., Yan, H., et al., (2017): MicroRNA expression signature and the therapeutic effect of the microRNA 21 antagomir in hypertrophic scarring. *Molecular Medicine Reports,* 15(3):1211-1221. Doi: 10.3892/mmr.2017.6104.

Ibrahim, S.F., Ali, M.M., Basyouni, H., et al., (2019): Histological and miRNAs postmortem changes in incisional wound. *Egyptian Journal of Forensic Sciences,* 9(1):1-6. Doi: 10.1186/s41935-019-0141-7.

Jenike, A.E. and Halushka, M.K., (2021): MiR-21: a non-specific biomarker of all maladies. *Biomarker Research,* 9(1):18. Doi: 10.1186/s40364-021-00272-1.

Li, G., Wu, W., Hoa, J., et al., (2018): Infiltration of immune cells and neuron apoptosis in brain after moderate burn injury: experiment with mice (in Chinese). *Chinese Journal of Emergency Resuscitation and Disaster Medicine,* 13:50-54. Https://caod.oriprobe.com.

Livak, k.j., and Schmittgen, T.D., (2001): Analysis of relative gene expression data using real-time quantitative PCR and the 2 (-Delta Delta C (T)) method. *Methods,* 25(4):402-408. Doi: 10.1006/meth.2001.1262.

Long, S., Zhao, N., Ge, L., et al., (2018): Mir-21 ameliorates age-associated skin wound healing defects in mice. *The Journal of Gene Medicine,* 20(6):e3022. Doi:10.1002/jgm.3022.

Lv, Y.H., Ma, K.J., Zhang, H., et al., (2014): A time course study demonstrating mRNA, microRNA, 18S rRNA, and U6 snRNA changes to estimate PMI in deceased rat's spleen. *Journal of Forensic Sciences,* 59(5):1286-1294. Doi: 10.1111/1556-4029.12447.

Lyu, H.P., Cheng, M. and Liu, J.C., et al., (2018): Differentially expressed microRNAs as potential markers for vital reaction of burned skin. *Journal of Forensic Science and Medicine,* 4(3):135-141. DOI: 10.4103/jfsm.jfsm_1_18.

Ma, L., Zhou, Y., Khan, M.A., et al., (2019): Burn induced microglia activation is associated with motor neuron degeneration and muscle wasting in mice. *Shock,* 51(5):569-579. Doi: 10.1097/SHK.0000000000001300.

Madea, B., Doberentz, E. and Jackowski, C. (2019): Vital reactions — an updated overview. *Forensic Science International,*305:110029. Doi: 10.1016/j.forsciint.2019.110029.

Malik, A.k., Khanna, k., Dhattarwal, S.K., et al., (2021): Histopathological evaluation of burn injury. *International Journal of Ethics, Trauma & Victimology,* 7(1):5-10. DOI: 10.18099/ijetv.v7i01.2.

Masson-Meyers, D.S., Andrade, T.A.M., Caetano, G.F., et al., (2020): Experimental models and methods for cutaneous wound healing assessment. *International Journal of Experimental Pathology,* 101(1-2):21–37. Doi: 10.1111/iep.12346.

Neri, M., Frati, A., Turillazzi, E., et al., (2018): Immunohistochemical evaluation of aquaporin-4 and its correlation with CD68, IBA-1, HIF-1α, GFAP, and CD15 expressions in fatal traumatic brain injury. *International Journal of Molecular Science,* 19(11):3544. Doi: 10.3390/ijms19113544

Peacock, J. and Peacock, P. (2020): Oxford handbook of medical statistics. 2nd Edition, Oxford University Press. United Kingdom. Doi.org/10.1093/med/9780198743583.001.0001.

Reddy, K.S.N. and Murthy, O.P. (2017): Thermal deaths. In: The essentials of forensic medicine and toxicology. 34th Edition, Jaypee Brothers Medical Publishers., New Delhi, p. 648. Doi: 10.5005/jp/books/18770_12

Salerno, M., Cocimano, G., Roccuzzo, S., et al., (2022): New trends in immunohistochemical methods to estimate the time since death: a review. *Diagnostics,* 12(9):2114. Doi: 10.3390/diagnostics12092114.

Sampaio-Silva, F., Magalhaes, T., Carvalho, F., et al., (2013): Profiling of RNA degradation for estimation of post mortem interval. *PLOS ONE,* 8(2): e56507. Doi: 10.1371/journal.pone.0056507.

Sangita, C., Garima, G., Jayanthi, Y., et al., (2018): Histological indicators of cutaneous lesions caused by electrocution, flame burn and impact abrasion. *Medicine, Science and the Law*, 58(4):216-221. Doi: 10.1177/0025802418776116.

Surendhar, P., Lakkawar, A.W., Uma, S., et al., (2023): Determination of postmortem interval (PMI) using histological changes in the cattle skin–A preliminary investigation. *Forensic Science International: Animals and Environments,* 4:100070. Doi: 10.1016/j.fsiae.2023.100070.

Suvarna, K.S., Layton, C. and Bancroft, J.D. (2018): Bancroft's Theory and Practice of histological techniques, 8th Edition, E book, *Elsevier Health Sciences,* Doi: 10.1016/C2015-0-00143-5.

Umapathi, A., Chawla, H., Singh, S.B., et al., (2023): Analysis of changes in electrolytes level in serum after death and its correlation with postmortem interval. *Cureus,* 15(5):e38957. Doi:10.7759/cureus.38957.

Vinay, J., Harish, S. Mangala, G.S., et al., (2017): A study on postmortem wound dating by gross and histopathological examination of abrasions. *The American Journal of Forensic Medicine and Pathology,* 38(2):167-173. Doi: 10.1097/PAF.0000000000000314.

Wang, J.L., Wang, X., Yang, D., et al., (2016): The expression of MicroRNA-155 in plasma and tissue is matched in human laryngeal squamous cell carcinoma. *Yonsei Medical Journal,* 57(2):298-305.
Doi: 10.3349/ymj.2016.57.2.298

Welson, N.N., Gaber, S.S., Batiha, G.E., et al., (2021): Evaluation of time passed since death by examination of oxidative stress markers, histopathological and molecular changes of major organs in male albino rats. *International Journal of Legal Medicine,* 135(1):269-280. Doi: 10.1007/s00414-020-02463.

Wilfinger, W.W., Mackey, K., Chomczynski, P. (1997): Effect of PH and ionic strength on the spectrophotometric assessment of nucleic acid purity. *Biotechniques,* 22(3):474-481. Doi: 10.2144/97223st01.

Zhang, K., Cheng, M., Xu, J., et al., (2020): MiR-711 and miR-183-3p as potential markers for vital reaction of burned skin. *Forensic Sciences Research,* 7(3):503-509. Doi: 10.1080/20961790.2020.1719454.

Zhang, Q.H., Chen, Q., Kang, J.R., et al., (2011): Treatment with gelsolin reduces brain inflammation and apoptotic signaling in mice following thermal injury. *Journal of Neuroinflammation,* 8:118. Doi: 10.1186/1742-2094-8-118.

Zhu, H.Y., Li, C., Bai, W.D., et al., (2014): MicroRNA-21 regulates hTERT via PTEN in hypertrophic scar fibroblasts. *PLOS ONE,* 9(5): e97114. Doi: 10.1371/journal.pone.0097114.

Zhu, S.X., Tong, X.Z. and Zhang, S. (2017): Expression of miR-711 and mechanism of proliferation and apoptosis in human gastric carcinoma. *Oncology Letters,* 14(4):4505-4510. Doi: 10.3892/ol.2017.677

How to cite this article: Ghobrial, M., Fouda, A., Abo Elwafa, S., Elnajjar, N., Refaat, O. (2025). Determination of the Burned Skin Injury Vitality and Its Postmortem Changes through Detection of Mir-711 and Mir-21 and Histopathological Changes in Adult Albino Rats. *Zagazig Journal of Forensic Medicine and Toxicology*, 23(1), 158-172. doi: 10.21608/zjfm.2025.329684.1203